# Digital twin integrating cell data for HPDC process modelling

Gariépy, A.; Pineau, F.



**Publisher's version / Version de l'éditeur:**

*Proceedings of the 2024 North American Die Casting Association Congress & Exposition, 2024-10-02*

# Digital twin integrating cell data for HPDC process modelling

A. Gariépy, F. Pineau
National Research Council Canada, Saguenay, Canada

## ABSTRACT

A single process cycle in high-pressure die casting involves a series of operations with complex flow, thermal, and metallurgical phenomena. Most commercial simulation software includes the mathematical framework to handle those. However, the user still needs to define a large number of coefficients to reproduce the magnitude of the physics and may also have to program functions to better replicate reality. This calibration effort can be an enabler for higher-fidelity simulations to efficiently develop new high-quality products, especially in the high-integrity field. This paper presents a data collection effort on a connected high-pressure vacuum die casting research and development cell that is fed into a process simulation. First, data was collected from the ladling robot, die casting machine, and spray actuator to provide an accurate representation of a typical cycle. Secondly, heat transfer behaviour was estimated for the cold chamber during pouring as well as for die spray to capture the heat exchanges in the system, as a complement to previously-acquired data for melt-to-die heat transfer. User functions were then programmed in ProCAST® to add the required features. Using this data, simplified cyclic simulations were run to calculate the expected steady-state die temperature regime and compare it to experimental data. Finally, a single-cycle flow and thermal simulation was run including the ladle pouring into the cold chamber. This works highlights some of the challenges and opportunities associated with a functional, off-line digital twin for high-pressure vacuum die casting, used as a tool to design new products and processes.

## INTRODUCTION

Smart manufacturing or industry 4.0 concepts are increasingly adopted as tools to optimize process productivity and quality. This generally involves a high level of digitalization of the operations, which includes sensors as well as modelling. One concept in industry 4.0 is the digital twin, a virtual replica of the process. Digital twinning is by itself a broad idea and there are many levels of digital twinning that can be characterized in terms of static or dynamic nature, as well as by the flow of information between the physical and numerical worlds[1, 2].

High-pressure die casting is a data-rich environment due to the numerous machines involved in automation[3, 4]. There is already extensive literature on collecting and analyzing data from specific components of HPDC equipment, such as injection units [5] or die spray[6]. One challenge with high-pressure die casting, especially in structural applications, is the number of sequential operations and equipment that each contribute to part quality at each cycle[7], which complicates the *a priori* choice of the relevant information to collect. While economically predicting the quality of individual castings based on process metrics only has proved challenging, this data remains valuable to detect equipment deviations[8, 9]. In both cases, the cell is an important data generator. In addition to common data acquisition hardware and software, such as National Instruments, programmable logic controllers have real-time access to the behaviour of the equipment under their control, sometimes with a very high data rate as for the shot control. As a single casting cell often involves multiple individual PLCs, a supervisory control and data acquisition (SCADA) system and network protocols such as OPC (Open Platform Communications) implemented on recent equipment enable grouping and synchronizing many data sources in real-time, albeit at a slower data rate. Finally, in addition to time-series numerical data, tools are also developed to analyze pictures or videos from the real world: this was applied for instance to quality control[10-12] or infrared imaging of the dies[13]. Such connected cells become a key element of real-time anomaly detection to help experienced operators monitor high-volume casting operations.

Process simulations are a critical and widespread tool in new product design, and there is wide public literature on the subject[14, 15], in addition to the extensive know-how that many users likely keep confidential. Although the numerical methods can vary[14-17], most commercial simulation platforms include the basic physical equations required to describe the process in terms of mass and heat flow. Commercial developers sometimes suggest "default" coefficients to use in process analyses. Many companies likely also have their own internal, undisclosed guidelines based on past experience with different die designs. Nevertheless, there are sometimes inconsistencies between chosen parameters, even in the public literature, that could affect the results and interpretation. For instance, heat transfer coefficients or functions between the melt and the die can vary by orders of magnitude in the literature[14, 18-22]. Similarly, heat loss in the cold chamber, which plays a key role on external solidification, has been described with different coefficients[14]. Finally, some parameters or coefficients such as the heat flow from die spray[14, 15, 23, 24] are rarely disclosed but are important factors on the stable temperature regime.

Simplifications are often made in process simulations to facilitate the analyses. For example, there exist several starting conditions for the melt in the shot sleeve. The simplest one is to consider that the sleeve is already prefilled with a motionless fluid, Figure 1a. The next level of complexity is to model the filling of the shot sleeve through an inlet over the pouring hole[14, 16], Figure 1b. In this case, the incoming flow is generally vertical and the hitting point depends on the inlet position which is defined by the user and generally fixed in time. Because the bottom wall of the sleeve is circular, the position of the hitting point is important as it will affect the resulting flow. The most complete approach that appears to recently gain interest in the literature is to model the kinematics of the ladle as it pours its content[25, 26] (Figure 1c). This adds the possibility of a richer description of the time-dependent flow rate, melt cooling as well as oxide formation in the ladle. This is also expected to produce a more representative temperature distribution in the shot sleeve.

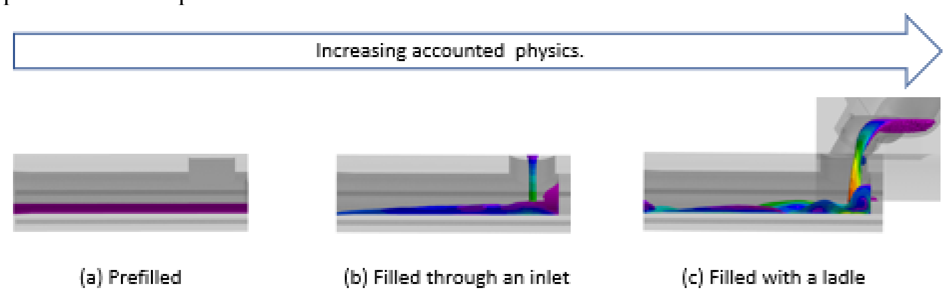


***Figure 1- Different approaches for shot sleeve initial condition calculation.***

Similarly, the thermal and solidification responses can be evaluated in different ways, from virtual dies to complete tooling models including thermal cycling before the filling analysis[14, 15]. The latter can be very complicated with intricate cooling channels, especially with conformal cooling, and die configurations to achieve the desired thermal stability.

Given the complex thermal, mechanical, and metallurgical physics involved in high-pressure die casting, data acquired on the casting cell can be very valuable to develop and validate simulations for predictive product and process design. The objective of this paper is therefore to present example applications of a connected cell in a small-scale research and development environment to improve large-scale process design and control. This instrumented platform provided accurate information on the equipment operations, using a combination of dedicated experiments on specific systems as well as full automated-cycle operations. Carefully measured inputs were used as much as possible to drive the numerical models; many numerical and physics parameters were still based on common modelling best practices and state-of-the-art in the literature. Actual outputs enabled verification or calibration of advanced process simulations. By integrating calibrated representations of many peripherals including die spray and ladle-based dosing, a complete process simulation was finally performed on a small prototype casting.

## EXPERIMENTAL METHODS

### HPVDC EXPERIMENTS

Experiments were conducted on the high-pressure vacuum die casting cell installed at the Aluminium Technology Center in Saguenay, Qc. A 530-ton Bühler SC N/53 die casting machine (Figure 2a) with a Fondarex HighVac/ExVac vacuum system is fed from a 700-kg furnace equipped for melt treatment. Dosing is made through a 6-axis ABB robot-mounted automatic ladling tool (Figure 2b). Die spray is performed by a dozen individual spray nozzles on a Rimrock linear actuator connected to pressurized tanks (Figure 2c). Thermal management uses three hot-oil circuits for the dies, heating cartridges for the shot sleeve, and cooling water for the plunger.


***Figure 2- (a) General view of the R&D cell, (b) robotized ladling tool, (c) die spray tool.***

This work leveraged a range of data collection methods that have been progressively implemented in this cell over the past five years. First, a National Instruments system was initially installed to gather event timing data from older equipment, temperature responses from in-die thermocouples, plunger and die spray actuator positions, as well as vacuum levels. This was complemented with the high-rate shot profiles that the Bühler DCM exports at each cycle. Following upgrades to the DCM and the cell controllers to newer programmable logic controllers, data acquisition was then expanded using the OPC (DA and UA, depending on the device) protocols. First, recipe and quality metrics were systematically collected on a shot-by-shot basis from the connected machines into a PostgreSQL database, for part-by-part traceability purposes. This capability was later expanded to continuously gather actual machine and robot states (at a relatively low frequency) and quality measurements from the Bühler and Fondarex systems. In parallel, additional flow sensors were installed on the die spray[6] and plunger lubricant peripherals to detect potential variations in operation, and connected either as analog input to the National Instruments system or over the network to the database.

In this work, two different tooling were used. Each was built as an insert pair, installed in the same die blocks and sharing the same shot sleeve, gating and overflows. The first one, illustrated in Figure 3a, is a simple stepped plate intended to characterize the cast material and measure the heat flow into and away from the die using a dedicated fast-response temperature sensor described in a previous paper[27]. The second one, shown in Figure 3b, is a slightly more complex 3D prototype designed to introduce typical features into a small envelope. In both cases, the structural Aural™-2 alloy was used in the experiments.

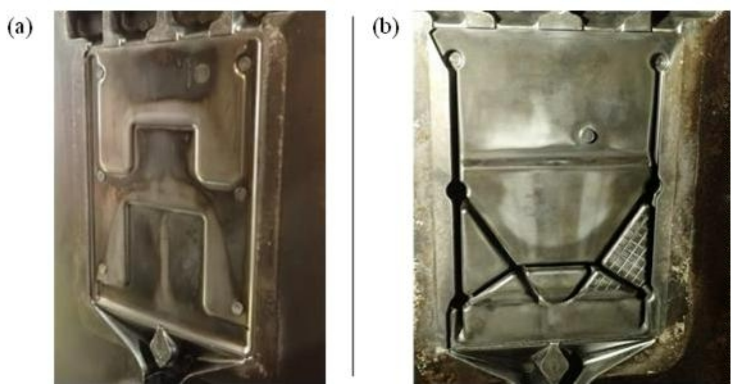


***Figure 3- (a) Stepped plate with fast-response temperature gradient sensor, (b) prototype tooling designed to introduced typical geometrical features.***

The fast-response temperature sensors in the stepped plate depicted in Figure 3a captured the die temperature gradient developing during solidification[22, 27] as well as the one generated during die spray. Using the same inverse heat transfer solution methodology, the heat flow extracted from the die by the water and lubricant spray was estimated as a function of time, to be used as input in the simulations. As shown in Figure 4, the calculated heat flow at a given location (a) varies with time as the nozzle rack (Figure 2c) travels across the die face following the recorded profile (b). While the absolute heat flow is not disclosed herein due to confidentiality, it was generally between different peak values reported in literature[23, 24]. It is worth noting that the actuator slowed down between programmed segments, leading to a jagged motion.

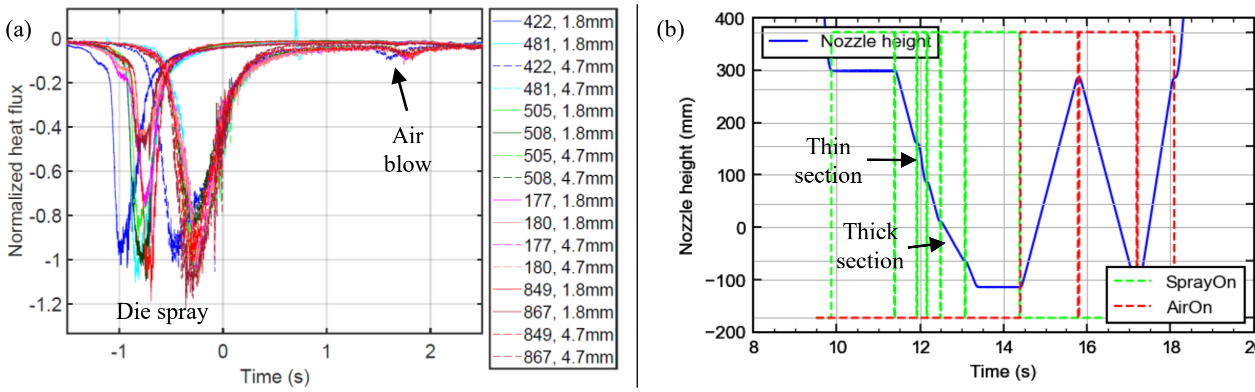


***Figure 4- (a) Calculated, normalized heat flux as a function of time during die spray at two locations, (b) typical spray actuator motion.***

Experimental measurements were also conducted on the thermal history before injection. As the melt is transferred from the furnace into the DCM, its temperature progressively decreases in the ladle and then inside the cold chamber. Efforts are often made to minimize heat loss during transfer by reducing transfer time or insulating the melt[28], but quantification of the heat loss during transfer is less widely considered[29]. This heat loss is however an important factor in temperature-related features and defects such as externally-solidified crystals, cold flakes, or cold shuts[20, 29]. An accurate representation of the melt temperature evolution from the furnace can therefore improve modelling reliability. In this investigation, two experiments were conducted to address this challenge. The first one involved measuring the melt temperature in the ladle during transfer to estimate temperature drop between the furnace and pouring position at the cold chamber, as shown in Figure 5a. While accurate time synchronization between data sources was not available at that time, the average melt temperature during pouring was estimated and used as an initial boundary condition in the simulations. Data was collected during a few cycles to preheat the ladle to a representative temperature, but metal build-up on the thermocouple increased its response time which made measurements progressively less reliable. The second experiment consisted in measuring the melt temperature evolution inside the cold chamber. The measurement method was based on literature[30] and included three 0.8 mm diameter thermocouples positioned in the melt along the length of the cold chamber as illustrated in Figure 5b. This experiment provided the data to iteratively reverse-engineer, at least approximately, the heat transfer conditions in the shot sleeve. This experiment was conducted on a pre-heated cold chamber, without prior casting cycles, and pouring was done manually over 3 seconds to roughly match the robotic ladling program. Melt temperature was also deliberately increased to provide a slightly wider measurement window before the onset of solidification. A dedicated setup with thermocouples embedded in the shot sleeve[29] would provide a more direct calibration of the time-dependent heat transfer, but was not feasible with the equipment available.

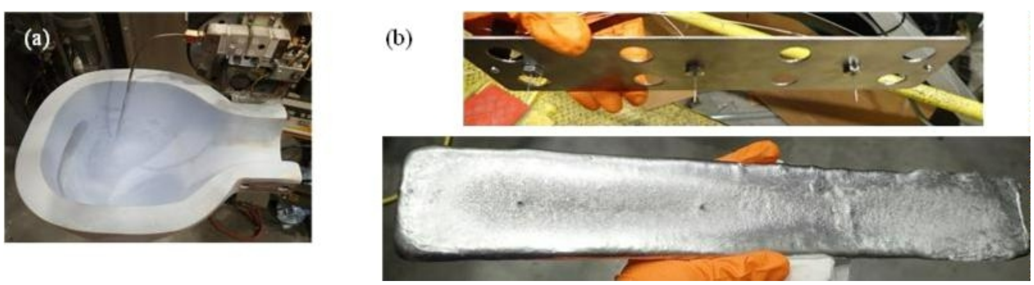


***Figure 5- Experimental setups for (a) melt temperature measurement in the ladle and (b) melt temperature evolution in the shot sleeve.***

Six-axis robots provide a lot of motion freedom and are a key element of many industrial cells (Figure 6a). In our facility, the cell controller was used as a bridge to gather high-rate position and orientation data of the tool center point (TCP) from the ladling robot: this provided extensive data to accurately model the pouring action into the shot sleeve. Replicating their motion in simulations can be a challenge, especially when the positioning of an existing robot with respect to the DCM is not well documented. In this investigation, 3D mockups were available individually from suppliers for the shot sleeve, the ladle and the robot, but not for their assembly. To accurately position the reported TCP with respect to the DCM referential, the relationship between the TCP coordinate system and the shot sleeve was reverse-engineered through metrology measurements using a Faro arm and a best-fit across three different measurement locations. This provided the robot path in space (Figure 6b-c) to validate to some extent the modelling accuracy for gravity pouring into the shot sleeve prior to the common filling simulation.

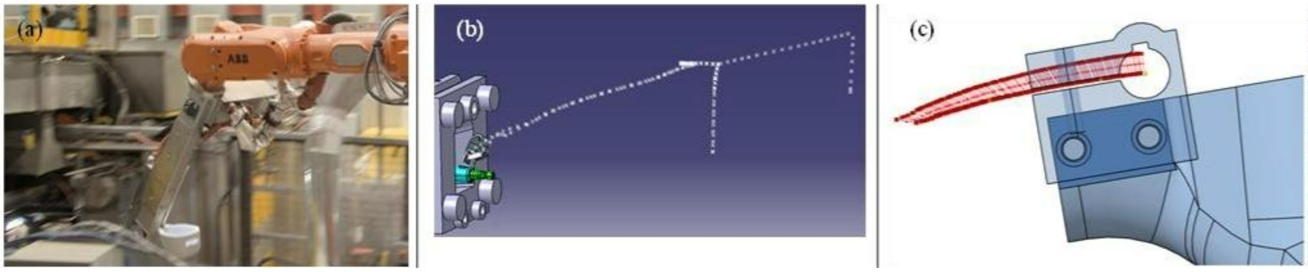


***Figure 6- (a) Ladling robot in the cell, (b) reported TCP points during a complete cycle, (c) detail of the pouring motion at the rotation axis.***

The second tooling (Figure 3b) was intended to replicate some representative industrial geometrical features to investigate their potential impact on the mechanical properties of the castings. This tooling was intended to produce a series of approximately 400 castings in relatively stable conditions while gathering part-traceable process data. Approximately 100 of these castings were selected to extract six tensile specimens per part. In parallel, the process data for a specific "average" part was taken as inputs to set up an "average" simulation with the cycle events timing, as summarized for example in Figure 7.

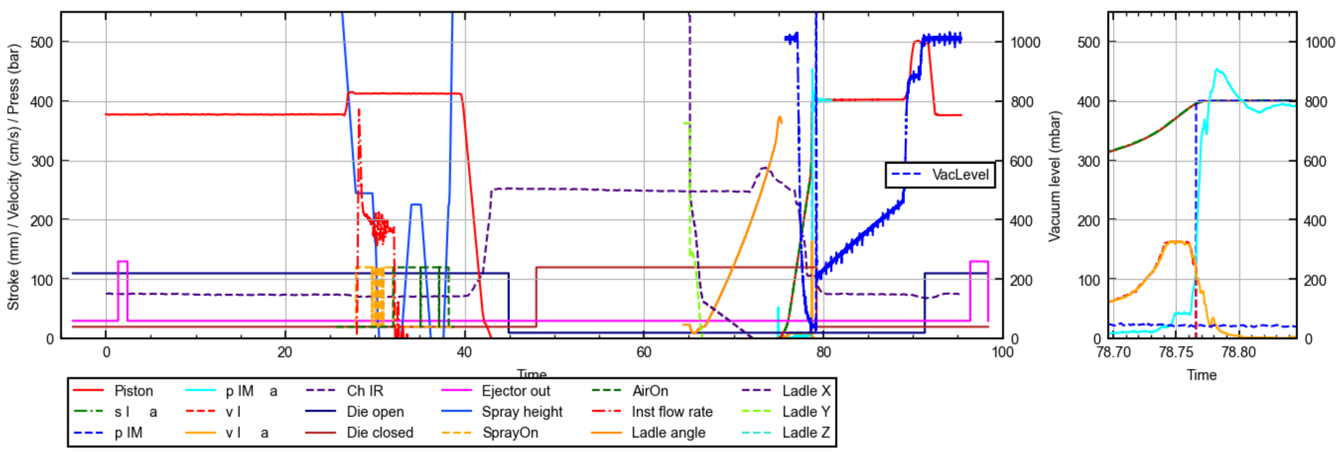


***Figure 7- Typical cycle recorded for analysis.***

## NUMERICAL MODELLING

Figure 8 depicts the 3D mockup and model of the stepped plate mold assembly, including all the geometrical features that were reproduced in the simulation. This model includes the volumes and interfaces required to capture the sequence of operations involved in a cycle. The simulation starts from metal in the ladle and therefore still does not account for upstream melt preparation operations that are also critical to quality[7].

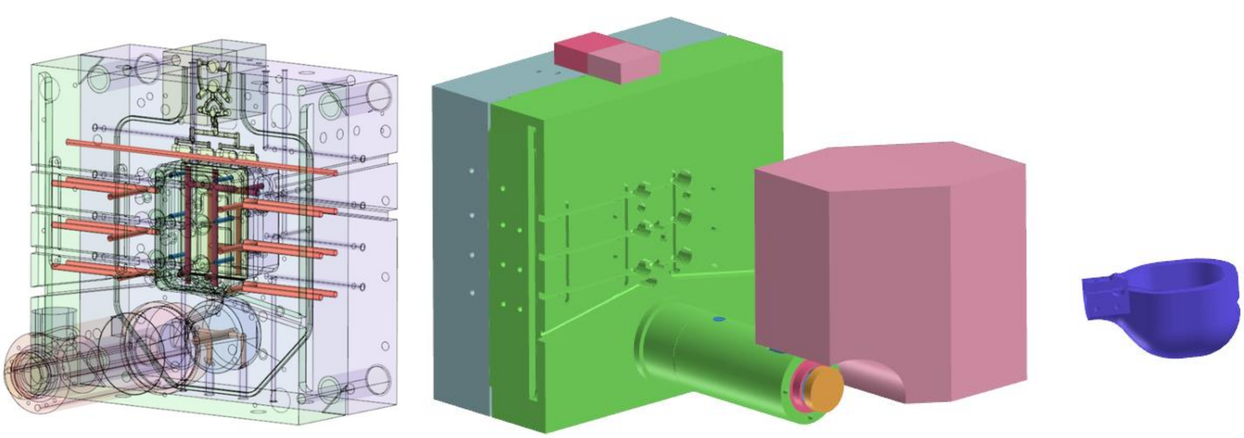

***Figure 8- Typical mold system representation considered in this work.***

## THERMAL CYCLING

The resulting condition of the part depends on how the melt flowed through the system, and the condition of the system depends on the way the melt passed through it in the previous cycles. The thermal condition of the tooling is the product of the repeated heat input from the melt, heat extraction from the cooling lines, and time-dependent heat extraction to the environment at the die faces. Similar to the physical process, the first step in modelling is to pre-heat the mold and perform several "injections" to allow the mold to reach a permanent cyclic regime[14].

Current modelling approaches include functions to consider all of the thermal phenomena involved in the casting process. One important step in some die temperature regulation strategies is the heat extraction by the spray and blowing phases. In software such as ESI's ProCast, this is done through the spray process condition where several nozzles with their trajectory could be defined via the graphical user interface (Figure 9)[14, 15]. The area covered by a moving nozzle could be a circle, a cone or a square. A heat transfer coefficient and ambient temperature are associated to this moving area. In the background, a time/space varying boundary condition for heat exchange is applied on selected element faces. In this work, as a heat flux cannot be directly defined, the convective heat transfer coefficient associated with the spray was calculated from heat flux measurements in Figure 4a, assuming a temperature of 20°C for the air-lubricant mixture and a mold surface temperature of 280°C. The estimated heat flux in front of the air nozzles during blowing was applied using the same methodology. The actual spray head motion in Figure 4 was positioned in the simulation referential and simplified as shown in Figure 9b. As this motion happens quickly, the time step needed to be small enough in order to catch the sharp temperature drop associated with the passage of the spray on each element. To avoid penalizing the global computation time, a variable time stepping strategy was employed with a maximum time step limit of 0.5 s for the global simulation and 0.01 s during the spray and blow phases.

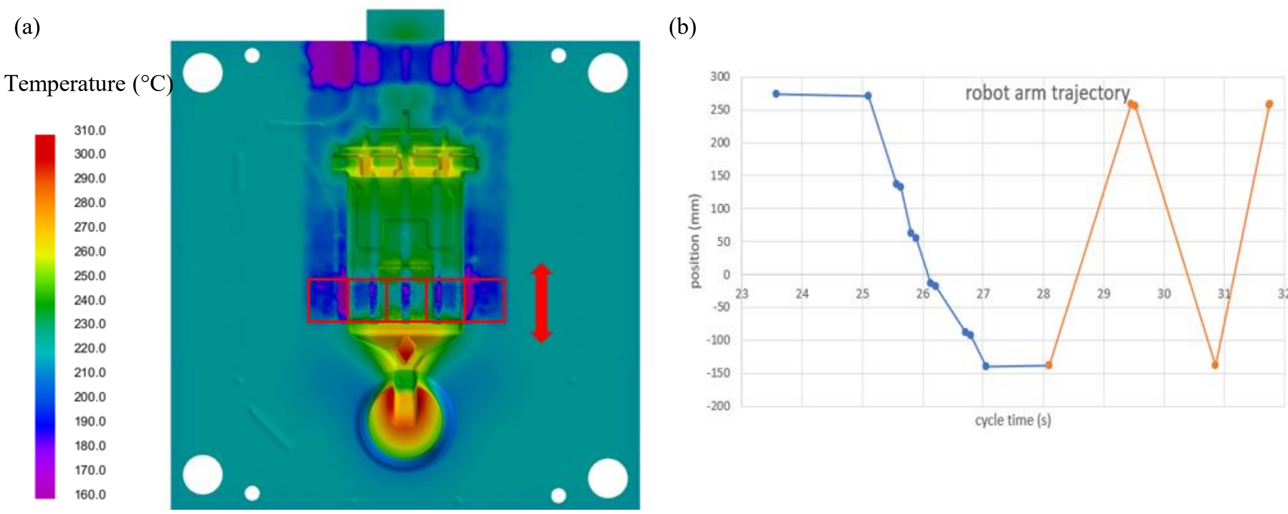


***Figure 9- Spray model set up in ProCast.***

Initial analyses (blue curve in Figure 10) showed that a constant heat flux applied on the projected surface yielded a sharp transition between the spraying area and the remaining surfaces of the mold and the temperature drop, and recovery was very fast compared to experimental measurements (red and orange curves for individual experiments). Furthermore, the background heat transfer coefficient during die spray on elements not directly impacted by the spray areas at a given time appeared too low: it would be expected to increase as spraying induces forced convection with air-mist entrainment. This suggests that this simplified spray representation may not account for all the phenomena.

To get more control over the spray boundary conditions and the freedom to implement any heat transfer distribution, a user function was defined, levering the software's built-in capabilities. To simplify the model, a global spray affected zone spanning the nozzle rack width was in our case appropriate, rather than defining separate nozzles. A Gaussian distribution, that can be skewed if necessary, appears to be more relevant for the cases discussed here. In addition to the direct heat extraction from the spray, it appears likely that there is a relatively strong secondary heat extraction below the spray target zone due to the downward flow of lubricant remaining on the surface (Figure 2c), compared to the background heat transfer to air. As a first approximation, the heat extraction pattern is believed to be similar to the heat extracted in a continuous casting process. A HTC of 500W/m$^2$K was subjectively set on an area below the direct spray area and the system is moving all together, as illustrated in Figure 11.

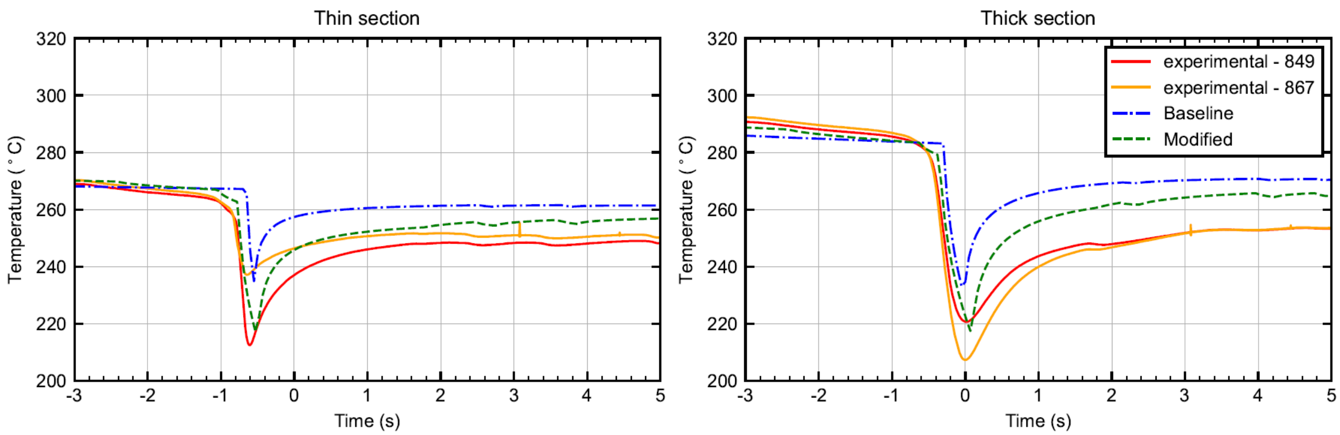


***Figure 10- Temperature evolution near the surface when spraying.***

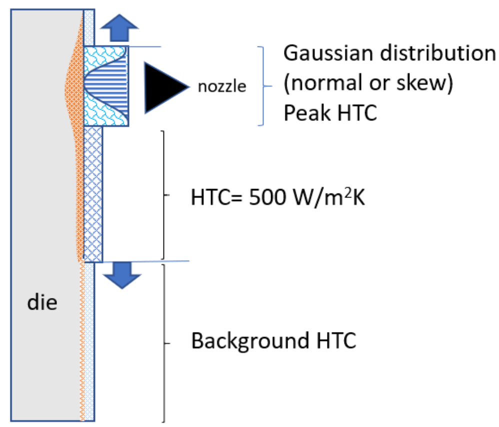


***Figure 11- Spatially-variable heat transfer pattern following nozzles programmed into user function.***

After several cycles, a repeatable state is developed. Computed temperature evolutions (green curves) compared to experimental ones are depicted in Figure 10. The slope of the temperature drop is generally well reproduced. However, the computed temperatures still recover too sharply and the magnitude of the temperature drop is still underestimated. This might be explained by the fact that further heat transfer by evaporation after the spray moved over the surface is not accounted for. Despite lower-than-actual heat extraction from spray model, predicted stable temperature cycles are consistent with experiments with the current assumptions. This suggests that the heat input from the casting may also be underestimated, leading to counter-balancing errors.

## LADLE POURING

Many process modelling software now permit to include the ladle in the model. This addition might be very useful when casting quality is at stake, especially in growing large-scale structural applications. As mentioned previously, the characteristics of the melt in the cold chamber represent the initial conditions of the injection. Modelling the ladle pouring is expected to introduce more heterogeneity in the melt compared to the conventional inlet simplification as the dynamics of the flow are slightly different.

In ESI's ProCast, the ladle approach was modelled as follows. A computational volume is added, adjacent to the shot chamber, to surround the ladle. The latter is initially empty and initially outside of this computational volume (Figure 12a). It is then translated to its reference position corresponding to the beginning of the pouring sequence and filled by means of a momentum source (Figure 12b-c) slightly above the pouring temperature. The challenge in this work was then to simultaneously translate and rotate the ladle around its rotation axis to reproduce the actual path retrieved on the physical cell (Figure 6). This was again achieved by means of a user function (Figure 12d) to numerically reproduce the kinematics of the actual ladle as it fills the shot sleeve by gravity.

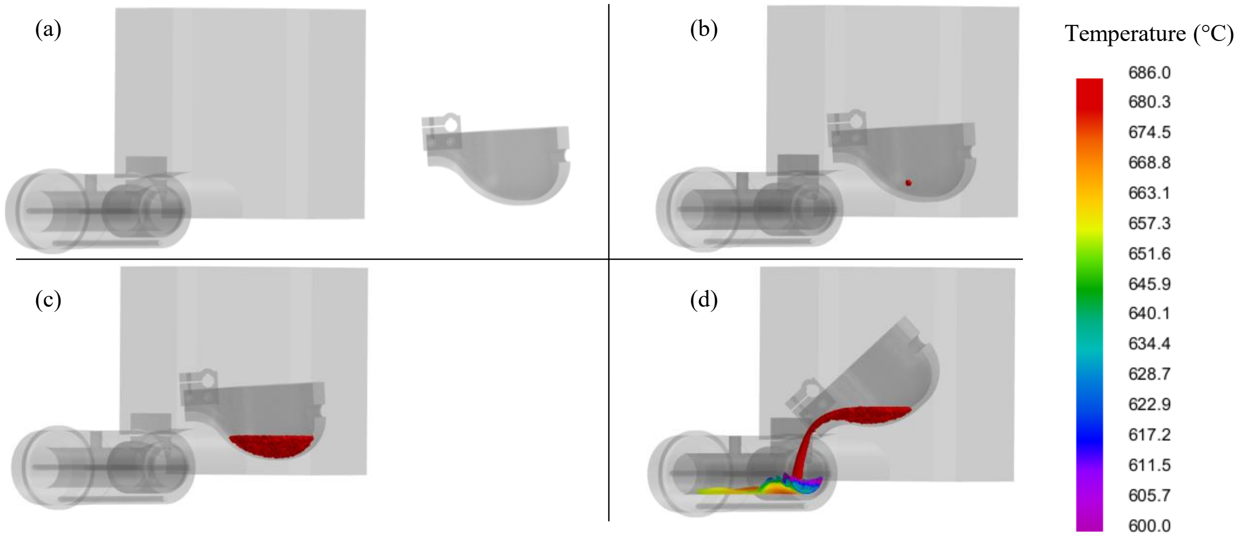


***Figure 12- Dosing model set up in ProCast.***

Figure 13a-b depicts a snapshot of the actual pour compared to the simulated one at a similar time. We observe that the simulated jet is thicker than actual and appears to deflect too much downwards. The relative coarse inter-penetrating meshes, dictated by the size of the model, does not seem accurate enough to catch the proper behavior of the pouring jet. The size of the 'fine mesh' is limited by the size of the problem and the boundary layer in the ladle is approximated by wall functions. The combination of inter-penetrating mesh technique, combined with volume-of-fluid (VOF) front tracking and wall boundary conditions adds to the complexity. In Figure 13c, we can observe that some fluid penetrates inside the ladle mesh. It was however not possible to validate how the wall boundary condition is treated in the solver. Different meshes and flow parameters were tried, including the more accurate "VOF" flow solver, but none of them significantly improved the accuracy of the pouring jet. It appears that the flow is too diffusive. As the model replicating the actual measurements led to melt flowing outside the cold chamber, the actual ladle motion was artificially modified in the model by bringing it closer to the pour hole to avoid metal loss. Refinement of the method could leverage optical quantification of the flow to fine-tune parameters such as viscosity[25]. Inclusion of the ladle inside the model represents nevertheless an advance compared to the classical "inlet approach".


***Figure 13- (a-b) Predicted and actual snapshot of the pouring operation, at a similar timestamp. (c) View of the predicted fluid behaviour and boundary in the interpenetrating mesh.***

Another important subject related to the shot sleeve is the heat transfer coefficient at the wall. A simplification with two zones having different heat transfer characteristics was selected as illustrated schematically in Figure 14a: heat transfer between the melt and the shot sleeve is expected to be more complex in reality, as the fluid velocity and viscosity continuously change in time and space, the surface finish can vary, and lubricant also plays a role[29]. Experimental values obtained by iterative, inverse modelling as shown in Figure 14b are slightly above those reported in the literature. Interpretation of the experimental data can prove challenging, as the thermocouple response time limits the validity of the early-stage results, and the melt waves appear to cause jagged temperature readings especially early on. While many combinations of pouring temperature and shot sleeve heat transfer coefficients could lead to similar results, independent calibration of each element should provide a more reliable representation of the process as a whole.

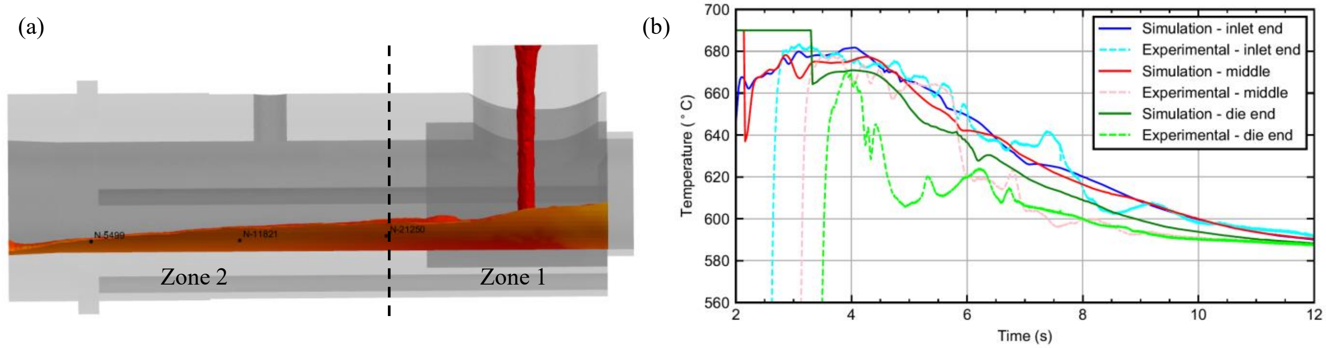


***Figure 14- (a) Simplification of the shot sleeve heat transfer coefficients as two zones, (b) comparison of experimental and calculated melt temperature curves used to estimate heat transfer coefficients.***

Combining the calibrated pouring step and heat transfer to the shot sleeve, Figure 15 depicts the main differences between the two dosing modelling approaches. The ladle is considered as an additional component with which the melt interacts. The melt is therefore losing heat from its free surface and through the ladle walls which implies that the average temperature of the melt in the shot sleeve is lower than when using the inlet BC with constant inflow temperature. Consideration of the ladle also implies that the relative oxide content will be higher in the shot sleeve, since an oxide skin is formed at the melt surface and poured inside the shot chamber (Figure 16). The dynamics of the flow are also different: with the ladle approach, we are dealing with a varying flow rate and flow direction while with the inlet, the flow rate is generally constant and unidirectional. Despite the greater modelling possibilities associated with the inclusion of the ladle in the model, many uncertainties still remain, including the challenge of accurately simulating the gravity-driven pour, and it should be used with caution.

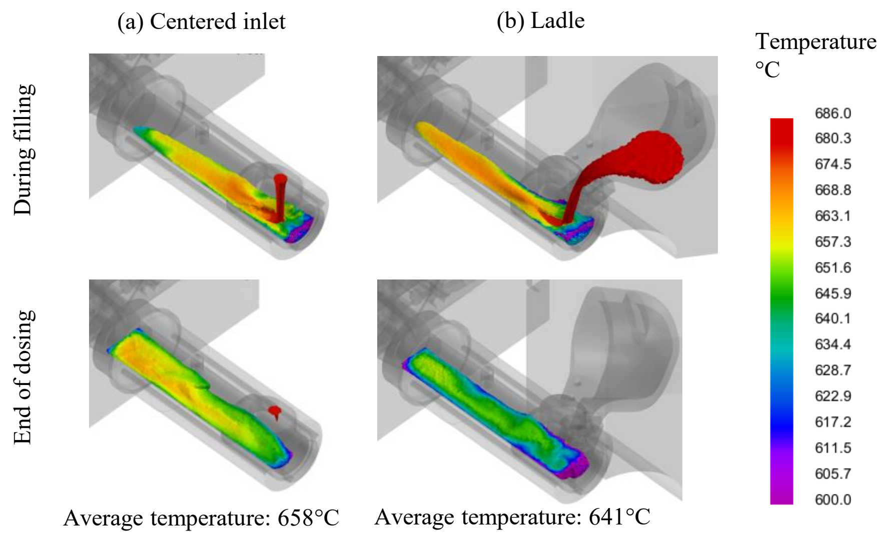


***Figure 15- Comparison of temperature distributions in (a) inlet and (b) ladle models.***

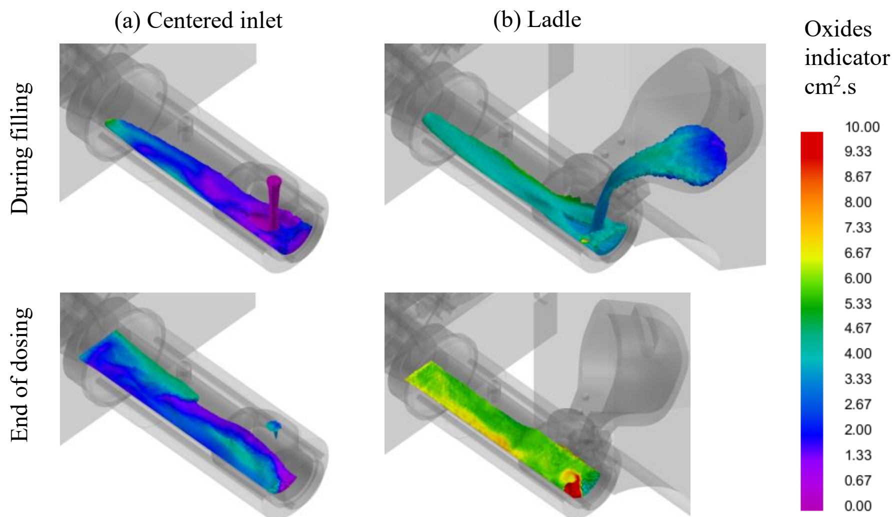


***Figure 16- Comparison of predicted oxides indicator during dosing step with (a) inlet and (b) ladle representations.***

Figure 17a-b shows the temperature distribution in the shot chamber just after filling. While the predicted average temperature of the melt at 614°C (Figure 17b) is above the liquidus, partial solidification occurs in the chamber especially close to the walls, and is responsible for the presence of externally solidified crystals (ESC) and cold flakes in the casting[31]. ESCs are expected to form in the chamber where the melt temperature drops below the liquidus, and are known to be transported into the cavity. Cold flakes are often associated with a high-solid-fraction layer that forms on the shot sleeve walls. Figure 17c shows such a crust of solidified alloy at the wall that likely corresponds to the folded features seen in a typical biscuit cross-section in Figure 17d. In ESI's ProCast, the reported solid fraction is related to the current temperature field only. Predicting directly the production and transport of ESC during the injection phase remains challenging with Eulerian numerical methods; this is one area where particle-based methods may be advantageous to follow the scraping of this solidified layer by the plunger and its potential transport into the casting[16, 32].

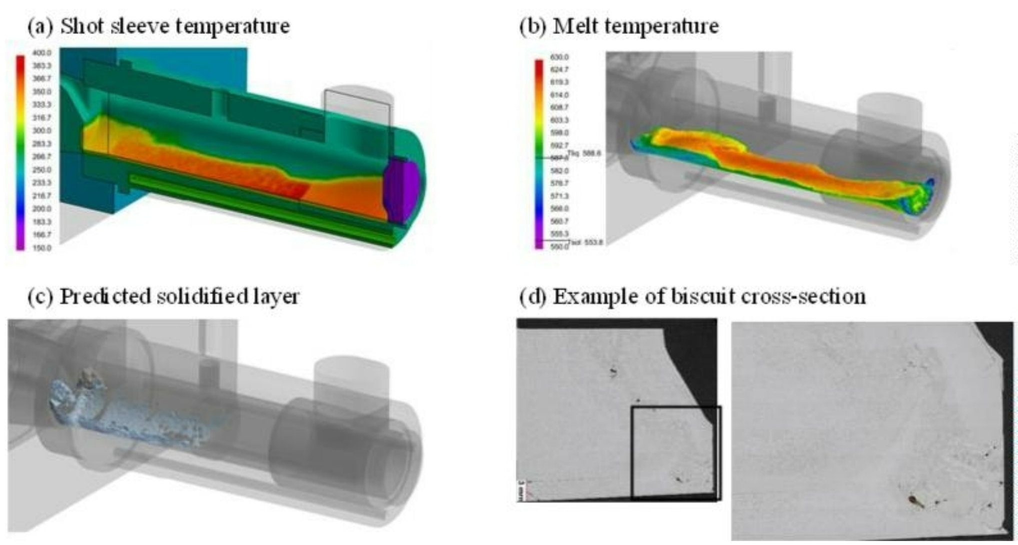


***Figure 17- (a-c) Calculated thermal and solidification response in the cold chamber, (d) Typical cross-section of a biscuit (bottom of chamber, at the plunger).***

## APPLICATION TO PROTOTYPE CASTING

The calibrated methods and coefficients derived from the dedicated experiments in the previous section were then applied to a different prototype casting. While the 3D shape introduces new challenges that were not specifically addressed herein, especially the view angles for the die spray, this work is intended as an example of peripherals integration to try to better predict part quality from the design stage.

A simulation for the prototype in Figure 3b was set up based on a typical cycle as shown in Figure 7, leveraging the building blocks developed for the spray and dosing functions. Some parameters such as the interfacial heat transfer function inside the cavity were taken from previous work done at the NRC[27]. Others, such as the coefficient describing the wall friction in the cold chamber and the cavity, were taken from the literature[14, 30].

A cyclic thermal analysis of the die was first conducted (Figure 18a). It should be noted that thermal cycling of the shot sleeve was performed through the use of time-dependent heat flux boundary conditions applied at the bottom surface of the chamber on two separate zones namely the pouring area defined by the sleeve insert and the remaining area of the sleeve. The filling and solidification simulation was then started from the ladle (Figure 18b).

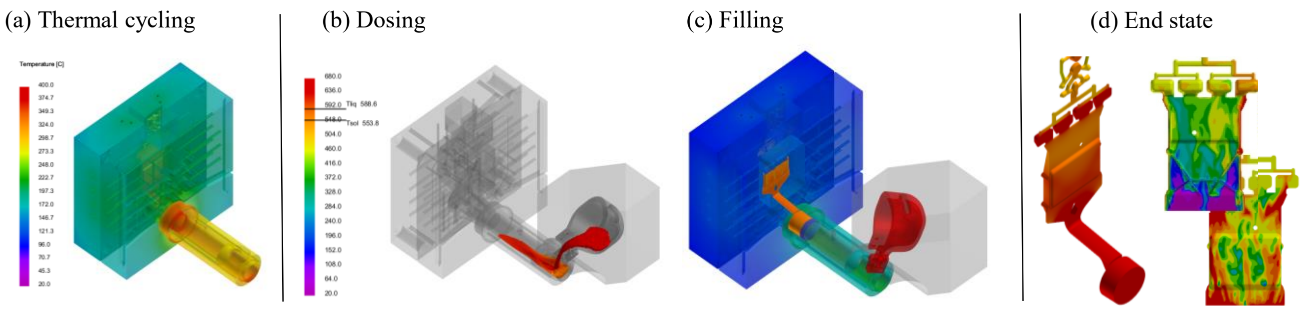


***Figure 18- Simulation steps for the prototype casting***

Typical quality indicator results such as temperature at end of fill, solidification time, air entrainment, oxides, porosity, etc. [33] were extracted from the results at the end of solidification (Figures 18d and 19) for each of the six locations that were subjected to mechanical testing. The fields were extracted for each gauge section of the tensile specimens, and post-processed for derived quantities such as averages and ranges within the sections. The purpose of this study was to correlate the predicted quality indicators to the measured average elongation at break at each location on this prototype, which is generally a challenge[33].

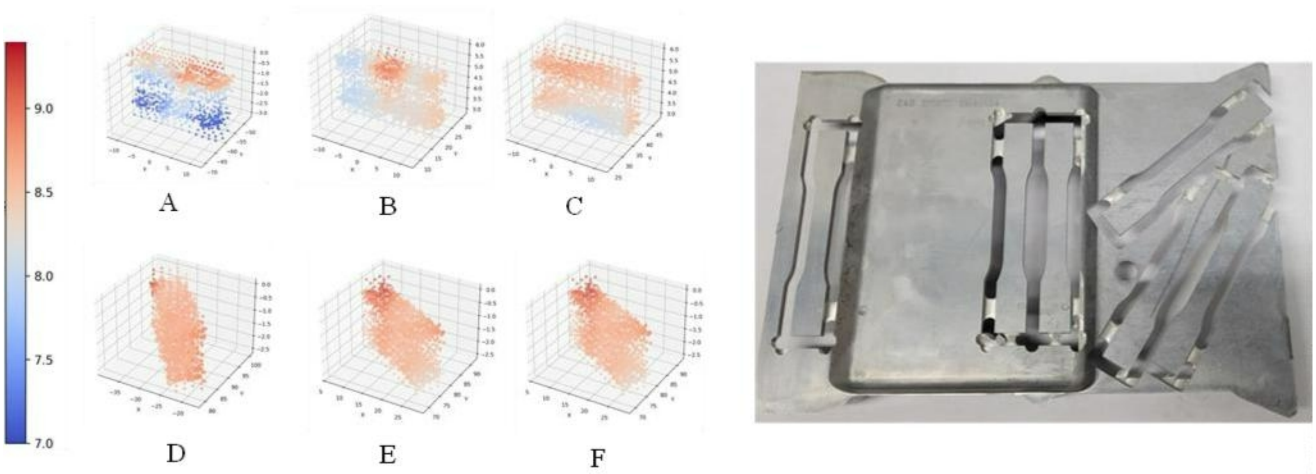


***Figure 19- Example of extracted results in gauge volumes***

While the experimental data set was limited in this investigation, some correlations could be established. Nevertheless, a wider investigation would be required to try to define a general model between predicted quality indicators and measured performance, especially for ductility metrics. The underlying numerical framework was however set up to try to capture more accurately the contributions of the cell peripherals in the complete cycle.

## CONCLUSION

Process simulation is an already well-established tool for die-cast product and process design. Continuous refinement of the simulations could be a key enabler to meet the requirements of continually more complex applications. First, calibration of individual coefficients and functions is a critical aspect to gain confidence and avoid potentially counter-balancing errors. Integration of peripheral operations in the analysis workflow could also contribute to the reliability of the results, going towards quantitative interpretation of the results beyond a comparative basis between iterations or similar products. The calibration effort can be significant, but the calibrated results can then be applied for simulation-driven optimization purposes. For instance, the dosing step in large castings involves moving a significant mass of metal to the cold chamber, and modelling could be a useful tool to optimize dosing before physical trials. Similarly, while minimal-spray applications are gaining interest with respect to water-based die spray, refinement of spray modelling could be applied to quantifying the deposition efficiency by tracking applicator motions.

Accurate process data, including both the inputs and outputs, is a key element of this calibration exercise, and a connected cell is a useful tool to meet this need as illustrated in this paper. A combination of traditional data collection and networked equipment, including PLCs and robots, provided rich data on many aspects of the process, and the same tools can also contribute to a process monitoring framework.

Some simplifying assumptions, which are difficult to verify, were still used herein and are still required to manage the computational cost. For instance, heat transfer coefficient between the impinging melt and the die cavity is likely to be a function of velocity, impact angle, and die lubricant[34], which are not accounted for in this work. Similarly, heat loss to the cold chamber during dosing and the first phase of injection is also likely to depend on the same factors.

Given the significant computation time compared to the fast pace of production operations, an evolved digital twin with 2-way, real-time data exchange between the physical and numerical worlds still appears challenging for the high-pressure die casting process. Nevertheless, there may be opportunities to integrate simplified representations, using finite element, analytical, or machine learning models, to refine process control for instance by allowing some forecasting capabilities based on current and recent data.

## ACKNOWLEDGMENTS

This work was carried out as part of a project supported by the NRC's METALTec industrial research and development group members and sponsors, as well as the NRC's Advanced Manufacturing Program. The work presented herein was part of a project funded by the Canadian Office for Energy Research and Development (2020-2023). The authors would like to acknowledge the contributions of the NRC team who participated in this study: Samuel Croft-Tremblay, Philippe Tremblay, Dany Drolet, Mario Patry, Dominique Bouchard, Michel Perron, Alexandre Morin, Jérémie Lavoie and Ramy Meziane, as well as the METALTec members and sponsors who contributed to this investigation and publication.

## REFERENCES

1. IBM. *What is a digital twin?* 2024; Available from: ibm.com/topics/what-is-a-digital-twin.
2. Uyan, T.C., et al., Industry 4.0 foundry data management and supervised machine learning in low-pressure die casting quality improvement. Int J Metalcasting. **17**(1): pp. 414-429 (2023).
3. Blondheim, D. "Artificial intelligence, machine learning, and data analytics: understanding the concepts to find value in die casting data". *NADCA Executive conference*. 2020.
4. Bonollo, F., N. Gramegna, and G. Timelli, High-pressure die-casting: contradictions and challenges. J Materials. **67**(5): pp. 901-908 (2015).
5. Bhowmik, S. and D. Blondheim, Time-series analysis and anomaly detection of high-pressure die casting shot profiles. Die Casting Engineer(November): pp. 14-18 (2019).
6. Blondheim, D. "Utilizing machine learning autoencoders to detect anomalies in time-series data". *North American Die Casting Association Congress & Exposition*. 2021. Indianapolis, IN.
7. Twarog, D., D. Apelian, and A. Luo, *High integrity casting of lightweight components (307)*. North American Die Casting Association (2016).
8. Blondheim, D., Improving manufacturing applications of machine learning by understanding defect classification and the critical error threshold. Int J Metalcasting. **16**(2): pp. 502-520 (2022).
9. Kopper, A.E. and D. Apelian, Predicting quality of castings via supervised learning method. Int J Metalcasting. **16**(1): pp. 93-105 (2022).
10. Parlak, I.E. and E. Emel, Deep learning-based detection of aluminum casting defects and their types. Eng Appl Artificial Intelligence. **118** (2023).
11. Zhang, B., et al., "A.I. vision system for automated casting quality inspection", in *North American Die Casting Association Congress & Tabletop*. 2023: Grand Rapids, MI.
12. Liu, D., et al., Digital twin and data-driven quality prediction of complex die-casting manufacturing. IEEE Transactions on Industrial Informatics. **18**(11): pp. 8119-8128 (2022).
13. David, B., Unsupervised machine learning and statistical anomaly detection applied to thermal images. Die Casting Engineer(November): pp. 8-18 (2018).
14. Dou, K., et al., A complete computer-aided engineering (CAE) modelling and optimization of high pressure die casting (HPDC) process. J Manuf Prc. **60**: pp. 435-446 (2020).
15. Bramann, H., et al., "Innovative product design and robust process layout in die casting with autonomous engineering", in *North American Die Casting Association Congress & Exposition*. 2018: Indianapolis, IN.

16. Tokunaga, H., Y. Motoyama, and T. Okane, Particle method simulation for formation and flow of cold flakes in high-pressure die casting. Int J Metalcasting. **13**(4): pp. 897-904 (2019).
17. Jakumeit, J., et al., Coupled modeling of misrun, cold shut, air entrainment, and porosity for high-pressure die casting applications. Light Metals: pp. 865-870 (2021).
18. Cao, H., et al., Direct observation of filling process and porosity prediction in high pressure die casting. Materials(12) (2019).
19. Long, A., et al., Determination of the heat transfer coefficient at the metal-die interface for high pressure die cast AlSi9Cu3Fe. Appl Thermal Eng. **31**: pp. 3996-4006 (2011).
20. Bhola, R. and S. Chandra. *Predicting castability of ultra thin-walled parts using simulations*. 2016; Available from: foundrymag.com/molds-cores/article/21928559/predicting-castability-for-thin-walled-hpdc-parts.
21. Gu, C., et al., Predicting grain structure in high pressure die casting of aluminum alloys: a coupled cellular automaton and process model. Comput Mater Sci. **161**: pp. 64-75 (2019).
22. Guo, Z.-P., et al., Development of thermal boundary condition model at metal/die interface of high pressure die casting process. Int J Cast Metals Res. **24**(3/4): pp. 151-157 (2011).
23. Sabau, A.S. and E.C. Hatfield, Measurement of heat flux and heat transfert coefficient due to spray application for the die casting process. Proc IMechE Part B: Eng Manuf. **221**: pp. 1307-1316 (2007).
24. Graff, J.L. and L.H. Kallien, "The effect of die lubricant spray on the thermal balance of dies". Chem-Trend, Inc.
25. Takada, K., et al., Direct observation and simulation of molten metal moving behavior during ladle pouring and plunger slow moving phase in die casting process. Int J Metalcasting. **17**: pp. 1149-1155 (2022).
26. Itakura, F., et al., Examination of variable tilting speed on flow behaviour during ladle pouring in die casting using SPH simulation. Int J Metalcasting (2024).
27. Gariépy, A., et al., "Solidification model calibration for predicting microstructure fields in HPVDC Aural(TM)-2", in *North American Die Casting Association Congress & Exposition*. 2021.
28. Liu, Y., et al., Enhanced mechanical properties and thermal conductivity of high-pressure die-cast AlMg6Si2MnZr alloy by controlling the externally solidified crystals. J Mater Process Technol. **306** (2022).
29. Helenius, R., et al., The heat transfer during filling of a high-pressure die-casting shot sleeve. Mater Sci Eng A. **413-414**: pp. 52-55 (2005).
30. Dou, K., et al. "Numerical simulation of fluid flow, solidification and defects in high pressure die casting (HPDC) process". *ICASP5-CSSCR5*. 2019. IOP Publishing.
31. Dou, K., et al., Understanding the initial solidification behavior for Al-Si alloy in cold chamber high-pressure die casting process combining experimental and modeling approach. Metall Mater Trans A. **53A**: pp. 3110-3124 (2022).
32. Pineau, F. and G. D'Amours, "Application of LS-Dyna SPH formulation to model semi-solid metal casting", in *8th European LS-Dyna conference*. 2011: Strasbourg, France.
33. Forsmark, J.H., et al., Using quality mapping to predict spatial variation in local properties and component performance in Mg alloy thin-walled high-pressure die castings: an ICME approach and case study. Integrating Materials and Manufacturing Innovation. **4**(6) (2015).
34. Cowell, T.L., et al., "Evaluation the thermal management performance of high-pressure die-casting lubricants utilizing the die lubricant splash test", in *North American Die Casting Association Congress & Tabletop*. 2022: Lexington, KY.